ACS Catalysis

Research Article

pubs.acs.org/acscatalysis

Atomically Dispersed Platinum on Gold Nano-Octahedra with High Catalytic Activity on Formic Acid Oxidation

Sungeun Yang and Hyunjoo Lee*

Department of Chemical and Biomolecular Engineering, Yonsei University, Seoul 120-749, Republic of Korea

Supporting Information

ABSTRACT: Platinum was epitaxially deposited on gold octahedral nanocrystals using an electrochemical method. The coverage of platinum on the gold surface was finely controlled from fully covered multiple overlayers (5 monolayers; denoted as ML) to atomically dispersed submonolayer (0.05 ML). Catalytic activity for formic acid oxidation increased significantly (0.52 A/mg_{Pt} for 5 ML to 62.6 A/mg_{Pt} for 0.05 ML) with decreasing coverage. This high activity resulted from the control of the reaction pathway toward direct oxidation producing no surface-poisoning species, induced by the absence of platinum ensembles and the bifunctional effect from neighboring Pt−Au sites. The distribution of atomically dispersed platinum was further confirmed by no activity for methanol oxidation, which necessitates platinum ensembles. This result exemplifies that a rational design of the catalyst nanostructure can lead to contrasting activities with the same catalyst, unprecedentedly high activity for formic acid oxidation vs no activity for methanol oxidation.

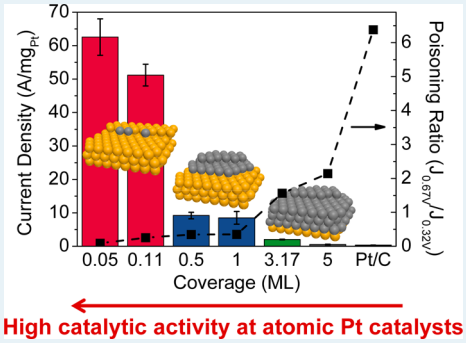

KEYWORDS: *nanocatalyst, Pt minimization, atomic catalyst, formic acid oxidation, Pt−Au*

INTRODUCTION

Platinum has been used as an essential catalytic substance in various fields, including fuel cells, the reduction of environmentally toxic compounds such as NO_x or CO, isomerization/cracking of hydrocarbon compounds in petroleum refineries, and so forth.[1−6] However, the high price and limited supply of platinum has motivated research for its more economic utilization. Reduction in the particle size of platinum has been generally applied for minimizing its use because smaller particle sizes of 1−3 nm provide more platinum atoms on the surface per unit mass, which maximizes the number of surface platinum atoms available for heterogeneous surface reactions. In addition to more exposed surface atoms, smaller nanoparticles have surface atoms with lower coordination numbers at step or edge sites, thereby increasing the activity per unit surface atom.

Recently, the shape control of platinum and platinum-based nanoparticle alloys has been explored to maximize the activity per unit surface platinum atom (specific activity). Various shapes of these nanoparticles, including cubes, octahedra, dendrites, and so forth, have been reported to have improved specific activity.[7−10] Shaped nanoparticles have a distinct surface atomic arrangement or modified electronic configuration, which facilitates the cleavage or recombination of chemical bonding and minimizes the contamination by spectator species on the surface.[11−14] However, these shape-controlled nanoparticles have usually been large (>10 nm in size) and have had a large percentage of platinum occluded inside the nanoparticles, thereby excluding them from the surface reaction. Although this shape control strategy has demonstrated interesting potential for platinum minimization through the control of nanostructure, its practical application will be delayed until the mass activity is significantly improved. Another interesting strategy for platinum minimization is single atomic catalysis, in which platinum atoms immobilized on supports are fully utilized for surface reactions. Zhang et al. reported the synthesis of a Pt_1/FeO_x catalyst in which the platinum atoms were separately dispersed on FeO_x supports, and this catalyst presented a high activity for CO oxidation.[15] However, the incipient wetness method was used to deposit the platinum; therefore, fine control over the amount of deposited platinum or the use of other types of supports could not be easily achieved.

Here, we report on the atomic-level utilization of platinum that was epitaxially deposited onto gold nano-octahedra. The amount of platinum deposited onto the well-defined Au(111) surface of the nano-octahedra could be finely controlled using an electrochemical method; Pt atoms, Pt islands, and Pt overlayers were prepared. The Pt atoms exhibited a very high mass activity of 62.6 A/mg_{Pt} for the electrocatalytic oxidation of formic acid. To the best of our knowledge, this activity is the highest value reported to date, and it is a few orders of magnitude greater than that of the commercial Johnson-Matthey Pt/C (0.37 A/mg_{Pt}). This high activity could be obtained through the control over the reaction pathway toward direct oxidation of formic acid.

Received: August 31, 2012
Revised: January 30, 2013
Published: February 5, 2013

   dx.doi.org/10.1021/cs300809j | *ACS Catal.* 2013, 3, 437−443

The electrocatalytic oxidation of formic acid follows direct ($HCOOH \rightarrow 2H^+ + CO_2$) and indirect ($HCOOH \rightarrow H_2O + CO_{ads}$) pathways. The indirect pathway generates surface poisoning species, CO_{ads}, at low potentials, which prohibits the oxidation of formic acid, whereas the CO_{ads} can be oxidized to CO_2 at high potentials. Therefore, voltammograms denoting current output over a wide potential range often show no current at low potential, and the current begins to appear at potentials >0.6 V (vs NHE) on platinum catalysts. To minimize the electrocatalytic reaction toward the indirect path, the ensemble of platinum atoms can be controlled. Neurock et al. have reported that the direct path only requires a single platinum atom, whereas the indirect path requires a larger surface ensemble (based on density functional theory simulations).[16] Sun et al. recently reported enhanced catalytic activity of tetrahexahedral Pt nanocrystals decorated with Bi adatoms by minimizing the surface platinum ensembles.[17] The surface ensembles were divided into smaller ensemble entities by adsorbing adatoms onto the platinum surface. However, this "adatom" method is not efficient because the adatoms block a significant amount of the catalytically active surface sites.

The enhanced activity for the oxidation of formic acid has been reported using various Pt−Au catalysts.[18−23] A few works have attributed the improvement in activity to the bifunctional effect where both Au and Pt participate in the formic acid oxidation. Although the complete oxidation of formic acid is difficult on gold (no formic acid oxidation was observed on bare gold surface in the condition we used in this work), the surface Au on Pt−Au catalysts promotes the dehydrogenation of formic acid and inhibits the dehydration that leads to the formation of CO.[18,19] Formate ($HCOO_{ads}$) was found to be a key intermediate for formic acid oxidation.[24] Possibly, the Pt−Au surface might help to prevent formate from being converted to poisoning CO_{ads} species. Therefore, to maximize the oxidation of formic acid toward the direct pathway, we deposited an atomic level of platinum onto a gold surface minimizing surface platinum ensembles and securing Pt−Au sites as much as possible.

EXPERIMENTAL SECTION

Preparation of the Working Electrode with Clean Au(111) Surface Using Gold Octahedral Nanoparticles. Gold nano-octahedra prepared by the recipe reported in ref 25 were dispersed in ethanol (99.9%, Duksan) after sufficient washing. Indium tin oxide (ITO) glass (<10 Ω/sq, Samsung Corning) was alternately cleaned by sonication with isopropyl alcohol (99.5%, Duksan) and deionized water (18.3 MΩ cm, Human Power II$^+$ Scholar, Human Corporation). The ITO glass was immersed in 10 vol % of 3-aminopropyltrimethoxysilane (APTMS, 97%, Aldrich) dissolved in methanol (99.8%, Duksan) for 1 day, which yielded an amine-terminated surface.[26] The gold nano-octahedra were immobilized onto the APTMS-modified ITO surface by immersing the APTMS-modified ITO glass in the gold nano-octahedra solution. Approximately 4 h were required to form a uniform gold nanocrystal layer on the APTMS-modified ITO glass. We previously reported the successful removal of the surface-capping agent from shaped gold nanocrystals.[27] The surface of the gold nano-octahedra was originally packed with a surface-capping agent; polyvinylpyrrolidone (PVP, MW 55,000). The PVP blocks the electron flow between the gold surface and the electrode. Four minutes of O_2 plasma treatment (CUTE, FEMTO Science) and subsequent cyclic voltammetry could remove the PVP layer while preserving the surface crystalline structure of gold. After the O_2 plasma treatment, high potentials were imposed using cyclic voltammetry to clean the fragments of PVP further. The ITO glass with cleaned gold nano-octahedra was taken out from the electrochemical cell and washed thoroughly with deionized water. Additional cyclic voltammetry was performed in a nitrogen-purged 0.1 M H_2SO_4 solution with a scan rate of 50 mV/s to confirm the clean and well-defined Au(111) surface structure of the gold nano-octahedra. Then, the electrode was thoroughly washed with deionized water and transferred into another cell to perform the platinum deposition.

Deposition of Platinum on Gold Nano-Octahedra with Controlled Surface Coverages. A conventional three-electrode electrochemical cell was used with a potentiostat (VSP, Bio-Logic), a platinum wire as a counter electrode, and a 3 M NaCl Ag/AgCl (RE-5B, BASi) electrode as a reference electrode. The ITO glass with the attached gold nano-octahedra was used as a working electrode. All of the electrochemical measurements were recorded and reported versus 3 M NaCl Ag/AgCl reference electrode (+0.209 V vs NHE).

To estimate the amount of charge required to form a platinum monolayer on the exposed gold surface, we related the charge of copper underpotential deposition (UPD) on the gold surface to the gold oxide reduction charge (Supporting Information, Figure S1). Figure S1a shows a typical cyclic voltammogram of gold, and the shaded cathodic peak indicates the reduction of the Au oxide species. Although integration of this peak has occasionally been used to estimate the surface area of gold,[28−34] this method is not very reliable. The gold oxide layer begins to form above 1.1 V, but the oxide layer often undergoes complicated reconstruction rather than forming a well-defined monolayer. It is difficult to determine the potential at which the gold oxide monolayer is formed and how long the high potential should be imposed to form it.[28] Furthermore, various forms of gold oxide species (Au−OH, Au_2O_3, and $Au(OH)_3$) can be formed on the surface;[29] consequently, the charge required to reduce the gold oxide varied from 386 to 723 $\mu C/cm^2$.[28−34] However, it is well-known that copper forms a monolayer on gold at a specific reduction potential.[35] Supporting Information, Figure S1b presents the cyclic voltammogram in the solution of 0.1 M H_2SO_4 + 10 mM $CuSO_4$ (≥99.99%, Aldrich). The peaks indicate that a copper monolayer is formed on the Au(111) surface.[35] When the lower potential was applied below 0.03 V, the deposition of bulk copper was observed. The shaded area in Supporting Information, Figure S1b denotes the oxidation of the deposited copper monolayer. The charge calculated from this area indicates the amount of charge required to form a copper monolayer on the gold surface. By correlating the charge calculated from the shaded area in Supporting Information, Figure S1a to the charge calculated from the shaded area in Supporting Information, Figure S1b, the amount of charge required to form a copper monolayer for a given gold surface can be estimated. When we compared the ratio of the charge measured from the gold oxide reduction peak to the charge measured from the copper UPD peaks for several samples, the ratio was constant as 2.983 with a standard deviation of 0.074. Because the copper remaining on the gold substrates can potentially pollute our experimental observations, we did not perform copper UPD for every sample but used this ratio of 2.983 to estimate the amount of charge required to form a

dx.doi.org/10.1021/cs300809j | ACS Catal. 2013, 3, 437−443

platinum monolayer (twice of the charge necessary to form a copper monolayer; $Pt^{4+} \rightarrow Pt$ vs $Cu^{2+} \rightarrow Cu$) for the given gold surface. For a working electrode prepared with the cleaned Au nano-octahedra, the cyclic voltammogram in a 0.1 M H_2SO_4 solution provides a gold oxide reduction peak. The charge for the gold oxide reduction can be calculated from the peak area, and the charge required for the formation of platinum monolayer can be estimated using the ratio of 2.983. The coverage of platinum on the gold surface can be calculated by dividing the actual charge imposed for platinum deposition by the charge required for the formation of platinum monolayer.

Platinum was deposited on the gold nano-octahedra by applying a constant voltage of 0.48 V in 10 μM H_2PtCl_6 (Aldrich) + 0.1 M H_2SO_4 solution. The voltage of 0.48 V and the platinum concentration of 10 μM were chosen to slow the rate of platinum deposition sufficiently. The amount of deposited platinum could be controlled by adjusting the deposition time. The amount of charge involved in the platinum deposition was used to determine the quantity of deposited platinum (Supporting Information, Figure S2).[36] The charge used for platinum deposition could be obtained from the shaded area in Supporting Information, Figure S2, then the mass of deposited platinum was calculated. The mass activity was determined by dividing the measured currents by the mass calculated.

CO Stripping. Electrochemical CO stripping was conducted to evaluate the platinum surface. The prepared working electrode (ITO/gold nano-octahedra/platinum) was immersed in a CO-saturated 0.1 M H_2SO_4 solution, and the potential was held at −0.147 V for 10 min. Then, N_2 gas was purged for 20 min to completely remove CO from the solution while the CO strongly attached to the platinum remained on the surface. After purging, linear sweep voltammetry was conducted from −0.147 to 1.05 V with a scan rate of 50 mV/s. A subsequent cyclic voltammogram was recorded to observe the surface oxidation/reduction and hydrogen adsorption/desorption on the platinum surface.

Electrocatalytic Oxidation of Formic Acid and Methanol. The oxidation of formic acid was performed by cyclic voltammetry in a 0.5 M HCOOH (~ 98%, Aldrich) + 0.1 M H_2SO_4 solution at a scan rate of 50 mV/s. The fifth scan was plotted after the CV was stabilized, and this fifth scan was sufficiently reproducible to compare various samples. Recorded data was normalized by platinum mass and platinum surface area. Platinum surface area was calculated from hydrogen adsorption area in cyclic voltammetry except 0.05 and 0.11 ML. In these two cases, platinum was not detected by hydrogen adsorption peak. All the platinum deposited electrochemically were assumed to be on the surface; then the corresponding area was calculated. The electrocatalytic oxidation of methanol was performed in the same manner using 0.5 M CH_3OH (99.8%, Aldrich) instead of HCOOH.

Reference Data Measured Using Pt Electrode and Commercial Pt/C. A platinum electrode was used as a working electrode to obtain bulk platinum data for CO stripping. The platinum electrode was finely polished with alumina powder and washed with deionized water before measurements. Supporting Information, Figure S3 shows CO stripping data for the Pt electrode. Twenty wt % Johnson Matthey Pt/C was used as commercial Pt/C catalyst. Two milligrams of Pt/C was dispersed in 0.5 mL of deionized water +1.5 mL of isopropyl alcohol (≥99.5%, Duksan) and sonicated for 20 min. Five microliters of this Pt/C dispersion was dropped and dried on a GC electrode (Pine Research Instrumentation) three times under a flow of nitrogen. A total of 3 μg of platinum was deposited on the electrode. This Pt/C-deposited electrode was used for the oxidation of formic acid or methanol under the same conditions as the ITO/gold nano-octahedra/platinum electrode.

RESULTS AND DISCUSSION

Platinum Deposition on Gold Nano-Octahedra. Gold octahedral nanocrystals (Figure 1a) immobilized on ITO glass were used as a working electrode for the electrochemical deposition of platinum and other electrochemical measurements. Our previous study demonstrated that the epitaxial overgrowth of the platinum layer was energetically favorable on the Au(111) surface, whereas the formation of platinum nanoclusters was preferred on the Au(100) surface.[27] The gold nano-octahedra provide a well-defined Au(111) surface for the epitaxial deposition of platinum. The nano-octahedra were originally covered with a polymeric capping agent (polyvinylpyrrolidone; PVP), which was inevitable for the shape control of gold nanoparticles; consequently, no electrochemical signal was observed before its removal. The PVP layer could be successfully removed by O_2 plasma and subsequent electrochemical stripping, while preserving the surface crystalline structure.[27] Figure 1b presents a cyclic voltammogram of the gold nano-octahedra, which exhibits a characteristic peak of the Au(111) surface at 1.33 V after the PVP was removed. Then, platinum was deposited onto the surface of the gold nano-octahedra by applying a constant voltage of 0.48 V in 10 μM H_2PtCl_6 + 0.1 M H_2SO_4 solution. A value of 0.48 V is a high potential, but it is barely adequate to reduce platinum; consequently, the deposition rate of platinum slowed because

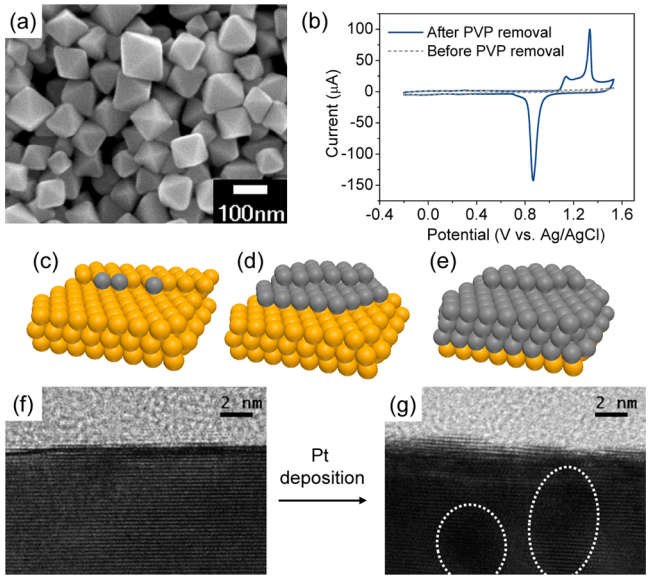

Figure 1. (a) SEM image of the gold nano-octahedra, (b) cyclic voltammograms for the gold nano-octahedra in 0.1 M H_2SO_4 solution with a scan rate of 50 mV/s before and after the removal of surface capping agent. Three models were proposed to describe the coverage-dependent properties of the platinum overgrown on the gold nano-octahedra; (c) Pt atoms, (d) Pt islands, and (e) Pt overlayers. HR-TEM images of (f) bare gold nano-octahedra and (g) 5 ML sample. *n* ML indicates that the amount of deposited platinum can form *n* monolayers on the gold supports.

dx.doi.org/10.1021/cs300809j | ACS Catal. 2013, 3, 437−443

of the weak reduction strength. Furthermore, the concentration of the platinum ion (10 μM) was chosen to ensure a slow platinum deposition. When the deposition rate was too fast, the deposited platinum formed aggregated nanoparticles rather than an epitaxial overlayer on the gold surface. The prepared samples were denoted as n ML, which indicates that the amount of deposited platinum can form n monolayers (ML) on the gold nano-octahedra. However, this nomenclature does not denote that the overgrown platinum formed smooth flat layers; instead, platinum islands were often observed, although the overgrowth was still epitaxial.

The platinum deposited on the gold nano-octahedra could be categorized into three models, depending on the surface coverage: Pt atoms (up to 0.1 ML), Pt islands (0.5 ML−1 ML), and Pt overlayers (above 3 ML). When platinum begins to deposit onto the gold surface at a slow rate, the platinum atoms diffuse until they are located at stable sites, such as steps or edges. Waibel et al. revealed by scanning tunneling microscopy images that platinum preferentially grows on the step sites of the gold surface.[37] At low coverage, the platinum atoms are stabilized at the step or edge sites of the gold surface (Figure 1c). The platinum atoms are well separated, and an ensemble, which can cause a reaction toward an indirect pathway, is rarely formed. Additionally, there is a large area of a bare gold surface, which can induce the bifunctional effect. When the coverage is higher, platinum islands form (Figure 1d). In this case, the ensemble consisting of many platinum atoms begins to form, but the bare gold surface is still available. As the electrochemical deposition proceeds further, platinum covers the entire gold surface by forming platinum overlayers (Figure 1e). Only platinum can be observed on the surface, and the gold is buried beneath the platinum. The bifunctional effect does not occur in this model. Figure 1f presents a high resolution TEM image of the bare gold surface, which shows a relatively smooth surface with a lattice spacing of 0.232 nm. When a 5 ML amount of platinum was deposited, the regular lattice was clearly observed with a spacing of 0.229 nm, which confirmed the epitaxial overgrowth of platinum on the gold surface. However, the surface became rougher, and black stains (denoted with white dotted lines in Figure 1g) appeared. The direct observation of platinum for lower coverage using electron microscopy was difficult to achieve because platinum has only one less electron than gold.

Characterization of Platinum Nanostructure Using Electrochemistry. Electrochemical CO stripping and consecutive cyclic voltammetry were conducted to gain deeper insight about the structure of the deposited platinum. The CO stripping peak is a measure of the CO adsorption energy and is highly dependent on the platinum nanostructure. For 0.05 ML (Figure 2a), the CO stripping peak (red line) was broad and relatively small. The earlier stripping peak from 0.4 to 0.7 V may result from CO adsorbed on the gold surface. The bare gold surface also showed a CO stripping peak in this range as shown in Supporting Information, Figure S4. When the coverage increased to 1 ML (Figure 2b), only the peak at 0.8 V became larger. The peak at 0.8 V likely arises from CO adsorbed on the platinum. However, 0.8 V is a quite high potential compared to 0.6 V for bulk platinum (Supporting Information, Figure S3). CO was more strongly bound to the Pt atoms and Pt islands deposited on the gold surface than to bulk platinum, which has also been reported in many previously published works.[23,38,39] When the coverage exceeded 3 ML (Figure 2c,d), the CO stripping peak potential exhibited a

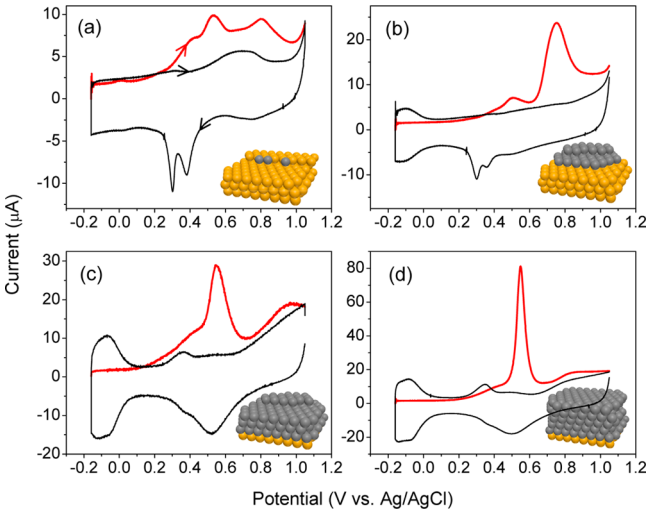

Figure 2. Linear scan voltammetry of CO stripping (red line) and subsequent cyclic voltammogram (black line) in 0.1 M H_2SO_4 solution with a scan rate of 50 mV/s for the (a) 0.05 ML, (b) 1 ML, (c) 3.17 ML, and (d) 5 ML samples.

negative shift to below 0.6 V, a peak position similar to that of bulk platinum. The 3.17 and 5 ML samples exhibit an interesting difference. The 5 ML sample presents a narrower and sharper peak, which indicates that the CO stripping characteristic is nearly the same throughout the platinum surface. The 5 ML sample has a more energetically uniform platinum layer than the 3.17 ML sample.

The cyclic voltammogram was recorded immediately after CO stripping, and it exhibited interesting features for the H adsorption/desorption and surface oxidation/reduction on the platinum surface. H adsorption/desorption peaks appeared between −0.16 and 0.1 V, which indicate the presence of platinum, and these peaks are usually used to calculate the amount of surface platinum because it is well-known that one hydrogen atom attaches to one surface platinum atom. However, in the 0.05 ML sample, there appeared to be no hydrogen adsorption, which strongly indicates an extremely small amount of surface platinum. When the coverage increased, the area of the H adsorption/desorption peaks became larger. The OH reduction peaks obtained with cathodic currents are also very interesting. Two distinct reduction peaks were observed at 0.3 and 0.4 V in the 0.05 ML sample. The typical Pt−OH reduction peak occurs at approximately 0.5 V, as in the 3.17 and 5 ML samples. The Au−OH reduction peak occurs at approximately 0.9 V, which was not observed in this case because Au−OH formation occurs after 1.1 V. Thus, the two reduction peaks at 0.3 and 0.4 V are new peaks that are neither Au−OH nor Pt−OH reduction peaks. These peaks did not appear when the same experiment was performed on bare gold nano-octahedra or bulk Pt electrode. These new cathodic peaks between 0.3−0.4 V have not been reported in previous studies. We assume that these new OH reduction peaks may result from interfacial OH located between gold and platinum and denote them as Au−Pt−OH peaks. The 1 ML sample presented two peaks at 0.3 and 0.4 V with a small plateau at approximately 0.5 V exhibiting both Au−Pt−OH and Pt−OH. For coverage above 3 ML, the Pt−OH peak became dominant, and only remnants of the Au−Pt−OH peaks appeared as a shoulder. Although the formation of Au−Pt−OH is assumed in the current stage, it is clear that the 0.05 ML sample (Pt atoms

dx.doi.org/10.1021/cs300809j | ACS Catal. 2013, 3, 437−443

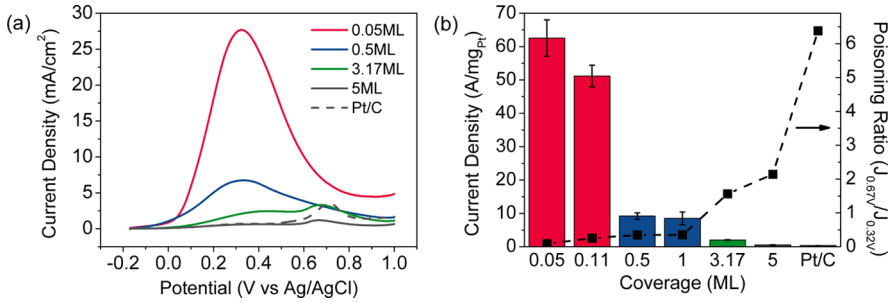

Figure 3. (a) Forward scan segments of the cyclic voltammograms showing the specific activities for 0.05 ML, 0.5 ML, 3.17 ML, 5 ML samples, and commercial Pt/C catalyst for electrocatalytic formic acid oxidation performed in 0.5 M HCOOH + 0.1 M H_2SO_4 solution with a scan rate of 50 mV/s, (b) comparison of the mass activities measured at 0.32 V and poisoning ratios, which is the current density at 0.67 V divided by the current density at 0.32 V.

model) and the 1 ML sample (Pt islands model) exhibited very different behavior from those with higher coverage (Pt overlayer model) or bulk platinum. X-ray photoelectron spectra were also measured for the 0.05 ML, 1 ML, and 5 ML samples (Supporting Information, Figure S5). The intensities of the Pt 4f peaks became larger as the amount of deposited platinum increased. The binding energies of the Pt $4f_{7/2}$ peak were 71.32, 70.95, and 70.90 eV for the 0.05 ML, 1 ML, and 5 ML samples, respectively. Although all of these energies fall into the region of metallic platinum, a slight modification of the electronic structure was observed depending on the coverage.

Electrocatalytic Formic Acid Oxidation. Figure 3 presents the results for the electrocatalytic oxidation of formic acid over the samples with various coverages. Whereas the direct pathway generates a current peak at ~0.3 V, the indirect pathway that produces the CO_{ads} poisoning species forms a current peak at ~0.7 V by oxidizing CO_{ads} to CO_2. The specific activity, which is the activity normalized by the area of surface platinum atoms, is shown in Figure 3a. It shows that Pt atoms or Pt islands have much higher activity than Pt overlayers or commercial Pt/C. The mass activity was compared by normalizing the oxidation anodic current at 0.32 V with platinum mass calculated from the charge imposed for the deposition of platinum. The 0.05 ML sample showed a very high mass activity of 62.6 A/mg_{Pt}. The previously reported highest value was 8.0 A/mg_{Pt} at a slightly different reaction condition.[40] The isolated Pt atoms deposited on the Au(111) surface resulted in a very high mass activity (e.g., 62.6 A/mg_{Pt} for the 0.05 ML sample and 51.2 A/mg_{Pt} for the 0.11 ML sample) because of the lack of Pt ensembles and the bifunctional effect. The Pt islands exhibited a significantly enhanced mass activity, which resulted mainly from the bifunctional effect (e.g., 9.2 A/mg_{Pt} for the 0.5 ML sample and 8.5 A/mg_{Pt} for the 1 ML sample). The Pt overlayers, which have a large quantity of Pt ensembles and no bifunctional effect, presented a considerably lower mass activity of 2.0 A/mg_{Pt} for the 3.17 ML sample and 0.52 A/mg_{Pt} for the 5 ML sample. As shown by the CO stripping results, 5 ML has energetically more uniform Pt layers with a lower platinum dispersion (surface atoms/total atoms) and a higher poisoning ratio, resulting in the poorer mass activity than 3.17 ML. Commercial Pt/C had a very low mass activity of 0.37 A/mg_{Pt}. The extent of poisoning was estimated by comparing the current from the indirect pathway with the current from the direct pathway. The poisoning ratio was calculated by dividing the current at 0.67 V by the current at 0.32 V. A higher poisoning ratio indicated that the oxidation of formic acid occurred through the indirect pathway. Whereas the samples with lower coverages have very small poisoning ratios, the samples with coverages greater than 3 ML and the commercial Pt/C presented much larger poisoning ratios. The oxidation of formic acid occurred by the direct pathway on the Pt atoms or Pt islands, but it followed the indirect pathway on the Pt overlayers or commercial Pt/C. The control over the pathway toward direct oxidation without surface poisoning species ensured the high mass activity. Long-term stability was also tested at 0.32 V (Supporting Information, Figure S6). The reduction in the current was the greatest for 0.05 ML, indicating that the stability of Pt atoms was poorer than Pt islands or Pt overlayers. The current was stabilized after 30 min, then the current of the atomically dispersed Pt was still much higher than the other cases.

Comparison of Bifunctional Effect and Electronic Modification Effect. Surely, the lack of Pt ensembles contributes to determining the reaction pathway toward direct oxidation. But there is ambiguousness whether it is a bifunctional effect or an electronic modification effect that plays an important role for controlling the reaction pathway, especially for the Pt islands model. To obtain further knowledge for formic acid oxidation on the Pt–Au system, two more types of platinum deposited on gold nano-octahedra were studied. First, a platinum monolayer with no bare gold surface was prepared (Pt monolayer). The Pt monolayer was deposited on gold nano-octahedra by using the UPD method as we previously reported.[27] The TEM image of the Pt monolayer on gold nano-octahedra and its formic acid oxidation result is shown in Supporting Information, Figure S7. The poisoning ratio of 1.7 indicates that the Pt monolayer favors the indirect pathway just like the Pt overlayers. Platinum atoms on the monolayer are located next to gold atoms; thus, the electronic modification by gold atoms will be similar to that in the 0.5 and 1 ML samples. However, the Pt monolayer favored the indirect pathway unlike the 0.5 and 1 ML samples indicating that the electronic modification is not an important factor determining a reaction pathway on the Pt–Au system. Rather, the availability of bare gold surface is more important. As the second sample, the bulk platinum was deposited on the corner sites of gold nano-octahedra with bare gold surface surviving on the facets (Pt bulk).[21] Its TEM image and the formic acid oxidation result is shown in Supporting Information, Figure S8. Platinum aggregates deposited on the corner sites of gold nano-octahedra have a diameter larger than 30 nm. In this case, we expect nearly no electronic modification of platinum by gold atoms. However, the Pt bulk favored the direct pathway with a poisoning ratio of 0.55. This result again emphasizes that the

dx.doi.org/10.1021/cs300809j | ACS Catal. 2013, 3, 437–443

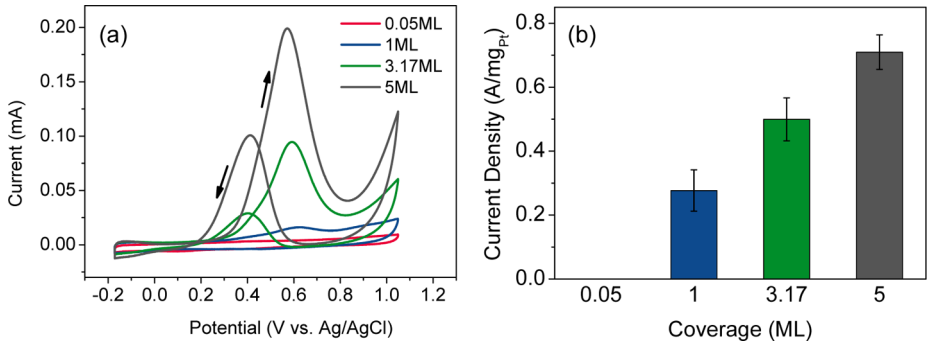

Figure 4. (a) Cyclic voltammograms for 0.05 ML, 1 ML, 3.17 ML, and 5 ML samples for electrocatalytic methanol oxidation performed in 0.5 M CH_3OH + 0.1 M H_2SO_4 solution with a scan rate of 50 mV/s, (b) comparison of the peak current densities in the forward scan.

electronic modification is not an important factor to determine the reaction pathway, but the availability of the bare gold surface is more important. In spite of the presence of large Pt ensembles, the bifunctional effect alone could control the reaction pathway toward direct oxidation. The similar trend with the Pt bulk was also observed on Pt-around-Au nanocomposites.[19]

Methanol Oxidation. On the other hand, the oxidation of methanol inevitably involves CO species as reaction intermediates. The CO species require surface platinum ensembles for further oxidation. The calculations based on density functional theory estimated that the primary pathway for methanol oxidation requires an ensemble size of between 3 and 4 platinum atoms.[16] Thus, if the 0.05 ML sample has no platinum ensembles with isolated platinum atoms on gold surface, it would show no activity for the oxidation of methanol. The platinum atoms might be connected in a chain at the steps or edges for the 0.05 ML sample, but the platinum domain would be too small to catalyze methanol oxidation. Figure 4 reveals that the oxidation of methanol actually did not occur on the 0.05 ML sample. The lack of methanol oxidation activity on the 0.05 ML sample strongly supports the supposition that the 0.05 ML sample actually consisted of isolated platinum atoms that were well dispersed on the gold surface. As the coverage increased, the methanol oxidation peak appeared and became larger. The CO stripping results in Figure 2 indicate that the CO was bound to platinum less strongly at higher platinum coverages. The weaker adsorption of the CO species would facilitate the oxidation of methanol with a lower peak potential and a higher peak current. The peak potential decreased to 0.63, 0.59, and 0.57 V, and the mass activity calculated from the peak current increased to 0.28, 0.50, and 0.71 A/mg$_{Pt}$ for the 1, 3.17, and 5 ML samples, respectively. Commercial Pt/C exhibited a mass activity of 0.66 A/mg$_{Pt}$, which was similar to that of the high coverage samples. Although the platinum submonolayer deposited on the gold nano-octahedra exhibited a very high activity for the oxidation of formic acid, this catalyst is not a good system for the oxidation of methanol. This finding indicates that the nanostructure of the catalyst should be tailored for the specific reaction to maximize its catalytic properties.

CONCLUSIONS

Platinum was epitaxially deposited onto gold nano-octahedra using electrochemical deposition. The amount of deposited platinum could be finely controlled from 0.05 to 5 ML. The 0.05 ML sample exhibited a very high mass activity for the electrocatalytic oxidation of formic acid and benefited from the lack of Pt ensembles and bifunctional effects of Pt−Au sites. The atomic level dispersion of platinum on the 0.05 ML sample was also confirmed by the lack of activity toward the oxidation of methanol. The 0.5−1 ML samples exhibited enhanced mass activity for the oxidation of formic acid, which mainly resulted from bifunctional effect. The samples with higher coverages had a large quantity of Pt ensembles and no bifunctional effect, thereby exhibiting low mass activity for the oxidation of formic acid that was comparable to that of commercial Pt/C. This study clearly shows that fine control of the nanostructure could maximize the activity for a specific reaction. Attempts to utilize cheaper conducting support materials that replace gold are currently in progress.

ASSOCIATED CONTENT

Supporting Information

Figures S1−S8; Copper underpotential voltammograms and chronoamperometry for Pt deposition, CO stripping data of bare gold surface and platinum electrode, XPS data, long-term stability data, TEM images and formic acid oxidation results for Pt monolayer and Pt bulk. This material is available free of charge via the Internet at http://pubs.acs.org.

AUTHOR INFORMATION

Corresponding Author

*E-mail: azhyun@yonsei.ac.kr. Phone: +82-2-2123-5759.

Notes

The authors declare no competing financial interest.

ACKNOWLEDGMENTS

This work was supported by the Basic Science Research Program (2012R1A1A2040791) and the Global Frontier R&D Program on Center for Multiscale Energy System (2011-0031575) through National Research Foundation of Korea funded by the Ministry of Education, Science and Technology.

REFERENCES

(1) Stamenkovic, V. R.; Mun, B. S.; Arenz, M.; Mayrhofer, K. J. J.; Lucas, C. A.; Wang, G. F.; Ross, P. N.; Markovic, N. M. *Nat. Mater.* **2007**, *6*, 241−247.

(2) Zhou, S. H.; Varughese, B.; Eichhorn, B.; Jackson, G.; McIlwrath, K. *Angew. Chem., Int. Ed.* **2005**, *44*, 4539−4543.

(3) Burch, R.; Breen, J. P.; Meunier, F. C. *Appl. Catal., B* **2002**, *39*, 283−303.

(4) Thormahlen, P.; Skoglundh, M.; Fridell, E.; Andersson, B. *J. Catal.* **1999**, *188*, 300−310.

(5) Bamwenda, G. R.; Tsubota, S.; Nakamura, T.; Haruta, M. *Catal. Lett.* **1997**, *44*, 83−87.
(6) Blomsma, E.; Martens, J. A.; Jacobs, P. A. *J. Catal.* **1997**, *165*, 241−248.
(7) Lee, H.; Habas, S. E.; Kweskin, S.; Butcher, D.; Somorjai, G. A.; Yang, P. D. *Angew. Chem., Int. Ed.* **2006**, *45*, 7824−7828.
(8) Kim, C.; Oh, J. G.; Kim, Y. T.; Kim, H.; Lee, H. *Electrochem. Commun.* **2010**, *12*, 1596−1599.
(9) Lim, B.; Jiang, M. J.; Camargo, P. H. C.; Cho, E. C.; Tao, J.; Lu, X. M.; Zhu, Y. M.; Xia, Y. N. *Science* **2009**, *324*, 1302−1305.
(10) Min, M.; Kim, C.; Yang, Y. I.; Yi, J.; Lee, H. *Phys. Chem. Chem. Phys.* **2009**, *11*, 9759−9765.
(11) Kim, D. S.; Kim, C.; Kim, J. G.; Kim, J. H.; Chun, H. H.; Lee, H.; Kim, Y. T. *J. Catal.* **2012**, *291*, 69−78.
(12) Bratlie, K. M.; Lee, H.; Komvopoulos, K.; Yang, P. D.; Somorjai, G. A. *Nano Lett.* **2007**, *7*, 3097−3101.
(13) Markovic, N. M.; Gasteiger, H. A.; Ross, P. N. *J. Phys. Chem.* **1995**, *99*, 3411−3415.
(14) Wang, C.; Daimon, H.; Onodera, T.; Koda, T.; Sun, S. H. *Angew. Chem., Int. Ed.* **2008**, *47*, 3588−3591.
(15) Qiao, B. T.; Wang, A. Q.; Yang, X. F.; Allard, L. F.; Jiang, Z.; Cui, Y. T.; Liu, J. Y.; Li, J.; Zhang, T. *Nat. Chem.* **2011**, *3*, 634−641.
(16) Neurock, M.; Janik, M.; Wieckowski, A. *Faraday Discuss.* **2008**, *140*, 363−378.
(17) Chen, Q. S.; Zhou, Z. Y.; Vidal-Iglesias, F. J.; Solla-Gullon, J.; Feliu, J. M.; Sun, S. G. *J. Am. Chem. Soc.* **2011**, *133*, 12930−12933.
(18) Zhang, S.; Guo, S. J.; Zhu, H. Y.; Su, D.; Sun, S. H. *J. Am. Chem. Soc.* **2012**, *134*, 5060−5063.
(19) Zhang, S.; Shao, Y. Y.; Yin, G. P.; Lin, Y. H. *Angew. Chem., Int. Ed.* **2010**, *49*, 2211−2214.
(20) Obradovic, M. D.; Tripkovic, A. V.; Gojkovic, S. L. *Electrochim. Acta* **2009**, *55*, 204−209.
(21) Min, M.; Kim, C.; Lee, H. *J. Mol. Catal. A: Chem.* **2010**, *333*, 6−10.
(22) Zhao, D.; Wang, Y. H.; Xu, B. Q. *J. Phys. Chem. C* **2009**, *113*, 20903−20911.
(23) Zhang, G. R.; Zhao, D.; Feng, Y. Y.; Zhang, B. S.; Su, D. S.; Liu, G.; Xu, B. Q. *ACS Nano* **2012**, *6*, 2226−2236.
(24) Cuesta, A.; Cabello, G.; Osawa, M.; Gutierrez, C. *ACS Catal.* **2012**, *2*, 728−738.
(25) Song, H.; Seo, D.; Park, J. C. *J. Am. Chem. Soc.* **2006**, *128*, 14863−14870.
(26) Jin, Y. D.; Dong, S. J. *Chem. Commun.* **2002**, 1780−1781.
(27) Yang, S.; Park, N. Y.; Han, J. W.; Kim, C.; Lee, S. C.; Lee, H. *Chem. Commun.* **2012**, *48*, 257−259.
(28) Trasatti, S.; Petrii, O. A. *Pure Appl. Chem.* **1991**, *63*, 711−734.
(29) Burke, L. D.; Nugent, P. F. *Gold Bull.* **1997**, *30*, 43−53.
(30) Friedrich, K. A.; Henglein, F.; Stimming, U.; Unkauf, W. *Electrochim. Acta* **2000**, *45*, 3283−3293.
(31) Ben-Ali, S.; Cook, D. A.; Evans, S. A. G.; Thienpont, A.; Bartlett, P. N.; Kuhn, A. *Electrochem. Commun.* **2003**, *5*, 747−751.
(32) Kumar, S.; Zou, S. Z. *Langmuir* **2007**, *23*, 7365−7371.
(33) Szamocki, R.; Velichko, A.; Holzapfel, C.; Mucklich, F.; Ravaine, S.; Garrigue, P.; Sojic, N.; Hempelmann, R.; Kuhn, A. *Anal. Chem.* **2007**, *79*, 533−539.
(34) Kiani, A.; Fard, E. N. *Electrochim. Acta* **2009**, *54*, 7254−7259.
(35) Herrero, E.; Buller, L. J.; Abruna, H. D. *Chem. Rev.* **2001**, *101*, 1897−1930.
(36) Uosaki, K.; Ye, S.; Naohara, H.; Oda, Y.; Haba, T.; Kondo, T. *J. Phys. Chem. B* **1997**, *101*, 7566−7572.
(37) Waibel, H. F.; Kleinert, M.; Kibler, L. A.; Kolb, D. M. *Electrochim. Acta* **2002**, *47*, 1461−1467.
(38) Liu, P. P.; Ge, X. B.; Wang, R. Y.; Ma, H. Y.; Ding, Y. *Langmuir* **2009**, *25*, 561−567.
(39) Kumar, S.; Zou, S. Z. *Langmuir* **2007**, *23*, 7365−7371.
(40) Wang, R. Y.; Wang, C.; Cai, W. B.; Ding, Y. *Adv. Mater.* **2010**, *22*, 1845−1848.